Lattice Defects in Microtubules: Protofilament Numbers Vary Within Individual Microtubules

D. Chrétien, F. Metoz, F. Verde,* E. Karsenti,* and R. H. Wade

Laboratoire de Biologie Structurale, CEA and CNRS URA 1333, DBMS/DSV, CEN-G, 85-X, 38041 Grenoble Cédex, France; and *European Molecular Biology Laboratory, Postfach 1022.40, D-6900 Heidelberg 1, Germany

Abstract. We have used cryo-electron microscopy of vitrified specimens to study microtubules assembled both from three cycle purified tubulin (3×-tubulin) and in cell free extracts of *Xenopus* eggs. In vitro assembled 3×-tubulin samples have a majority of microtubules with 14 protofilaments whereas in cell extracts most microtubules have 13 protofilaments. Microtubule polymorphism was observed in both cases. The number of protofilaments can change abruptly along individual microtubules usually by single increments but double increments also occur. For 3×-tubulin, increasing the magnesium concentration decreases the proportion of 14 protofilament microtubules and decreases the average separation between transitions in these microtubules. Protofilament discontinuities may correspond to dislocation-like defects in the microtubule surface lattice.

It is well known that in vitro polymerization of tubulin yields microtubules with a range of protofilament (pf)[1] numbers. Depending on the assembly conditions, most microtubules have 13 or 14 pfs (6, 7, 22, 24, 31), but, using thin sectioning of tannic acid–stained microtubule pellets, forms with from 8 to 17 pfs have been observed (1, 31). The precise mechanisms which determine the pf numbers of in vitro assembled microtubules are not understood. Factors which have an influence include, the incubation temperature (Pierson, G. B., and P. R. Burton. 1975. *J. Cell Biol.* 67:336a.), the buffer type, the pH and purification procedure (31), the presence of microtubule-associated proteins (7), the presence of nucleating templates (18, 35), or the cell origin of the microtubule protein (1). Whatever the causes of this structural polymorphism, it is usually thought that, in vitro as well as in the cell, individual microtubules have a fixed number of pfs which is determined at the microtubule nucleation stage (18, 35).

In previous work using cryo-electron microscopy of vitrified specimens we have shown that the pf number in individual microtubules can be determined directly from their characteristic image contrast (11–13, 51). In the case of in vitro assembly, this provides a much more efficient method of determining microtubule pf numbers than was previously possible using thin sectioning. We now use this method to show that the number of pfs varies within individual microtubules for samples assembled both from three cycle purified beef brain tubulin and in cell free extracts from *Xenopus* eggs.

Address correspondence and reprint requests to Dr. Wade.

Dr. Chrétien's present address is European Molecular Biology Laboratory, Postfach 1022.40, D-6900 Heidelberg 1, Germany.

1. *Abbreviations used in this paper*: pf, protofilament; 3×-tubulin, three cycle purified tubulin.

Materials and Methods

Isolation of Microtubule Protein and Preparation of Cell Extracts from Xenopus Eggs

Microtubule protein from beef brain was isolated by three cycles of assembly–disassembly according to standard methods (3, 20). 3×-tubulin was exchanged into 100 mM Pipes, 1 mM $MgCl_2$, 1 mM EGTA, pH 6.7 by a centrifugation–filtration method (20). The protein concentration was determined by the Lowry method as modified by Peterson (29), and was routinely controlled by OD_{280} measurements. The protein content of 3×-tubulin was assessed by SDS-PAGE on 7.5% polyacrylamide gels (T = 7.5%, C = 2.7%). The protein concentration was adjusted to 6 mg/ml, 20 mM acetyl phosphate, 1 mM GTP, 0.5 μg/ml acetate kinase, and 1 mM $MgCl_2$. Protein samples were divided into 500 μl aliquots and stored frozen before use.

Xenopus egg extracts were prepared according to published procedures from activated eggs incubated 90 min in cycloheximide (40).

Preparation and Observation of Vitrified Samples

Microtubule assembly is temperature dependent and we have found that precautions are needed to maintain the temperature of the specimen droplet when it is placed on the electron microscope grid before rapid freezing. All the preparation steps were carried out with the specimens protected by a plexiglass panel and under a hood to reduce air currents and cooling due to the liquid nitrogen bath. The most important precaution was the use of a simple controlled environment device, shown in Fig. 1, to regulate the temperature and humidity around the 4-μl sample droplet, thereby preventing self cooling due to evaporation (11).

Three cycle purified tubulin (3× tubulin) samples were thawed just before use, divided in two 250-μl aliquots, transferred to pre-cooled microcuvettes and left on ice for 15 min. Assembly was initiated by warming the samples to 37°C; one in a water bath and the other in the constant temperature chamber of a Uvikon 930 (Kontron Instruments, Milan, Italy) recording spectrometer. The polymerization was followed by the absorbance changes at 350 nm.

We used holey plastic/carbon–coated 400-mesh copper grids with the aim of forming a thin layer of vitreous ice spanning the holes (15). Grids were lightly glow discharged in air before use. Specimens were prepared at different time points along the polymerization plateau and were observed

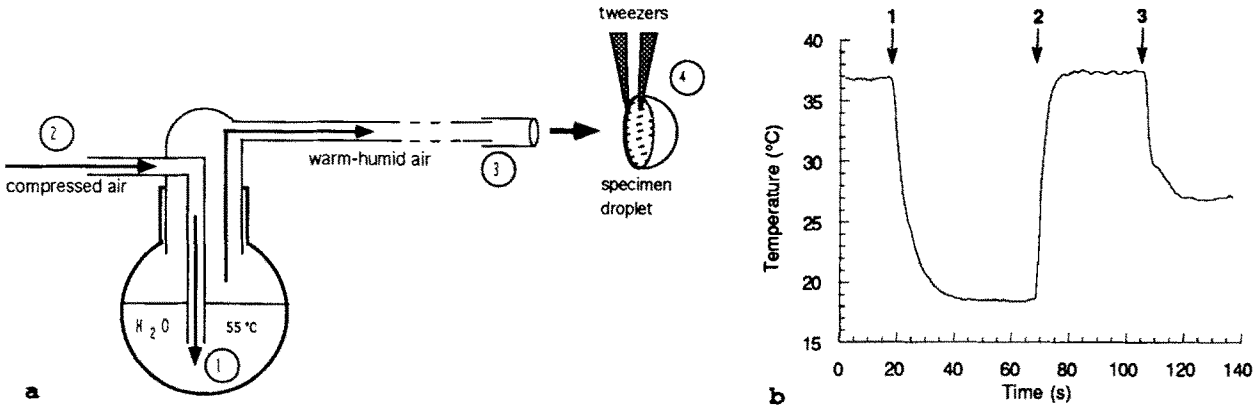

Figure 1. (*a*) Environmental device used to regulate the specimen temperature during the preparation of vitrified specimens. (*1*) Source of warm humid air; (*2*) Compressed air flow; (*3*) Teflon tube; (*4*) Grid held by tweezers attached to the guillotine device. (*b*) Use of the device to regulate the temperature of the 4-μl droplet. The droplet temperature was recorded using a fine thermocouple coupled to an x-y recorder. The beginning of the plot indicates the temperature of the droplet regulated to 37°C using the environmental device. After 20 s the warm humid air flow was directed away from the specimen (*1*). The temperature fell by 18°C and stabilized at around 19°C. This corresponds to 8.5°C below room temperature (27.5°C). The warm humid air flow was again directed towards the specimen (*2*). The temperature jumped rapidly to 37°C. Small temperature variations of $\pm$0.2°C were due to the bubbling system. The thermocouple was then removed from the specimen droplet and dried with a filter paper (*3*). The thermocouple recorded the room temperature which was 27.5°C.

using an electron microscope (Carl Zeiss, Oberkochen, Germany). Images were recorded at magnifications in the range 16,200 to 31,200× using the usual low dose methods (36). Electron microscope magnifications were calibrated using the position of the (40 Å)$^{-1}$ layer line in the computed Fourier transform of the microtubule images. When examining the effects of magnesium, the images were recorded at 18,600× so as to allow the longest possible stretches of individual microtubules to be followed whilst still maintaining the clearly visible fringe contrast.

Interphasic *Xenopus* egg extracts were incubated at room temperature to induce microtubule assembly in the absence of added nucleating sites. Specimens for electron microscopy were again prepared using the controlled environment device, since regulated humidity around the sample was essential to prevent evaporation. Without this precaution the droplet self-cooled to some 8°C below room temperature. Specimens were observed in an electron microscope (EM 400; Philips Electronic Instruments, Eindhoven, Netherlands) operating at 80 kV.

Characterization of Microtubule Populations

For the selected assembly times, three good quality images were chosen from the available set and prints of the entire micrographs (9.7 by 8 cm) were made at a final magnification of 60,000. The pf numbers in all microtubules were identified using the image contrast characterizations previously described (11–13, 41). The total lengths of the different microtubules were measured on the prints using a small calibrated wheel. The length over which individual microtubules could be followed on single prints was limited to an average of 3.5 μm by the film size and the magnification used to record the micrographs. Transitions from one microtubule type to another were counted. Defining the pf number along a given stretch of microtubule as N and the increment/decrement across a transition region as in the transition frequencies were determined by dividing the number of transitions from an N to an N $\pm$ m pf configuration (m = 1 or 2) by the measured microtubule length in the N pf configuration. The inverse of the transition frequency gives the "average separation" between transitions in the N pf microtubules.

Image Analysis

Micrographs, magnification 18,600, were digitized using a CCD Pulnix camera with a pixel size corresponding to steps of 5.6 Å at the specimen. The image data were transferred to a Vaxstation 3200 computer. The image processing, except inverse Fourier–Bessel transforms, was carried out using the Semper 6P program package.

80 × 80 pixel arrays were extracted from the digital array, and after orientation, projections were made along the length of the microtubule axis. The resulting intensity profiles were compared to previously accumulated profiles and similar profiles from the same microtubule region were averaged and Fourier transformed. Based on the theory of helical reconstructions (21) the equatorial amplitudes and phases were used to calculate cross-sections through segments of the microtubules. These cross-sections help assessment by giving a direct visual representation of the pf number at different positions along the microtubule and complement the direct identification using the image contrast. No attempt was made to correct for the contrast transfer function since we are comparing neighboring regions of the same microtubule for which the imaging conditions are identical. For the cross-section calculations, an initial estimate of the number of pfs N is obtained from the microtubule image contrast (11–13, 41). To check this choice of N, the reconstructed cross-section is calculated using Bessel orders n ranging from N − 2 to N + 2. The reconstructions using Bessel orders n = N − 1 and n = N + 1 can always be rejected because they are found to have a significant imaginary part, and of course, the cross-sections must be real. We find that the pfs appear connected around the inner wall only when n = N, they are disconnected for n = N − 2, and for n = N + 2 they appear as spike-like protrusions from a smooth inner core. Consequently the criterion for selecting the correct value of N is that the calculated cross-sections be both real and connected around the inner wall, as with previous three dimensional reconstructions (2, 4).

Results

Microtubules Assembled from 3×-Tubulin

Fig. 2 is an overall view of vitrified microtubules which, in defocused electron micrographs, are imaged as long ribbon-like structures some 25- to 30-nm wide. Each microtubule image has broad and strongly contrasted edge fringes and

Figure 2. Micrograph showing a typical view of vitrified microtubules which have the characteristic contrasts of the indicated numbers of pfs. The correspondence between image contrast and pf number are to be found in references 11–13, 41. Transition regions from one type of image contrast to another within the same microtubule are marked by double arrows. The different contrasts indicate that the pf number changes within the microtubule. The contrast associated with flattened microtubules can be seen at some cross-over regions marked by stars.

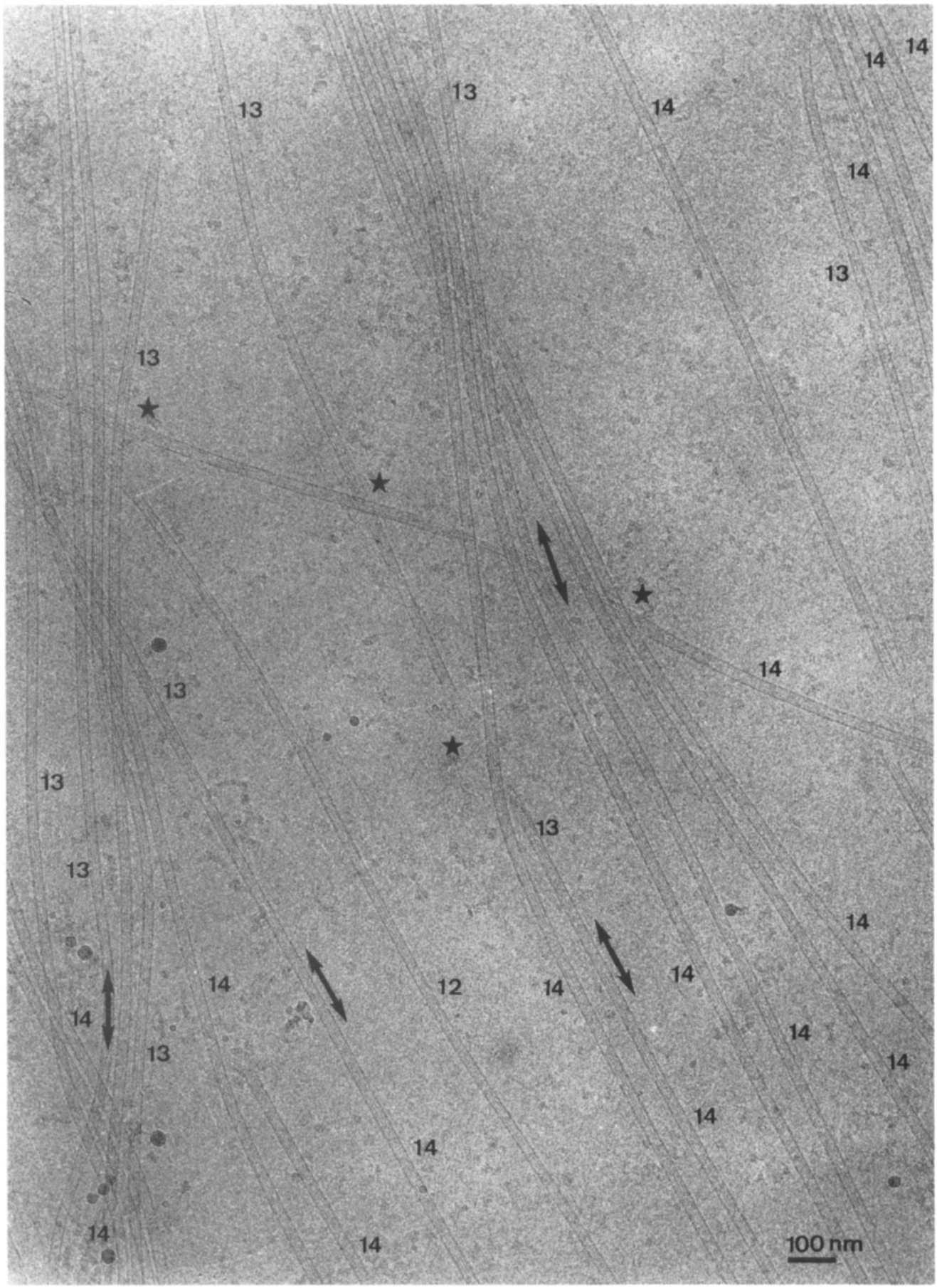
14
14
13
13
14
14
13
13
13
14
13
13
13
13
14
14
14
12
14
14
14
13
14
14
14
14
14
100 nm

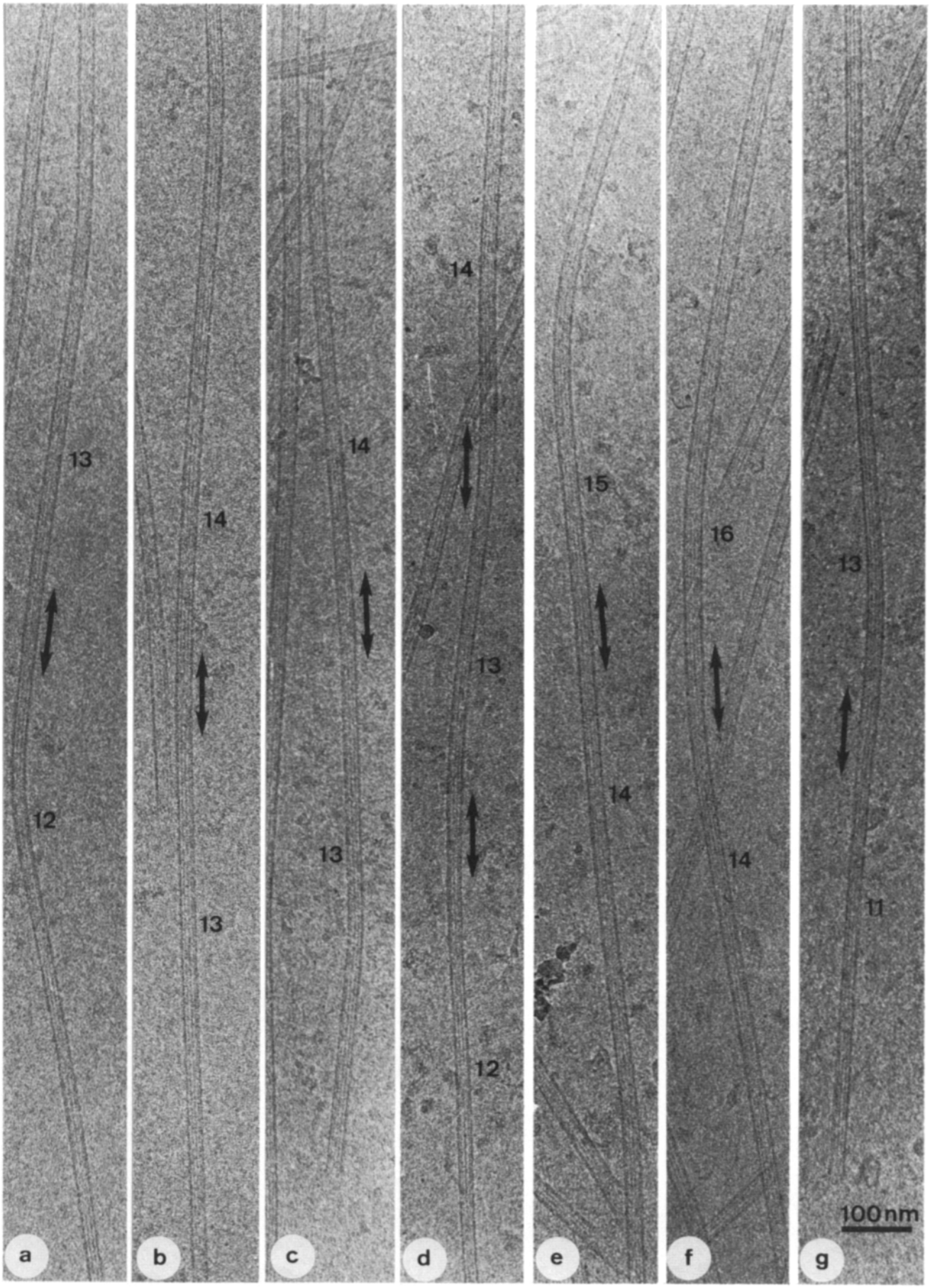
13
12
a
14
13
b
14
13
c
14
13
12
d
15
14
e
16
14
f
13
11
g
100nm

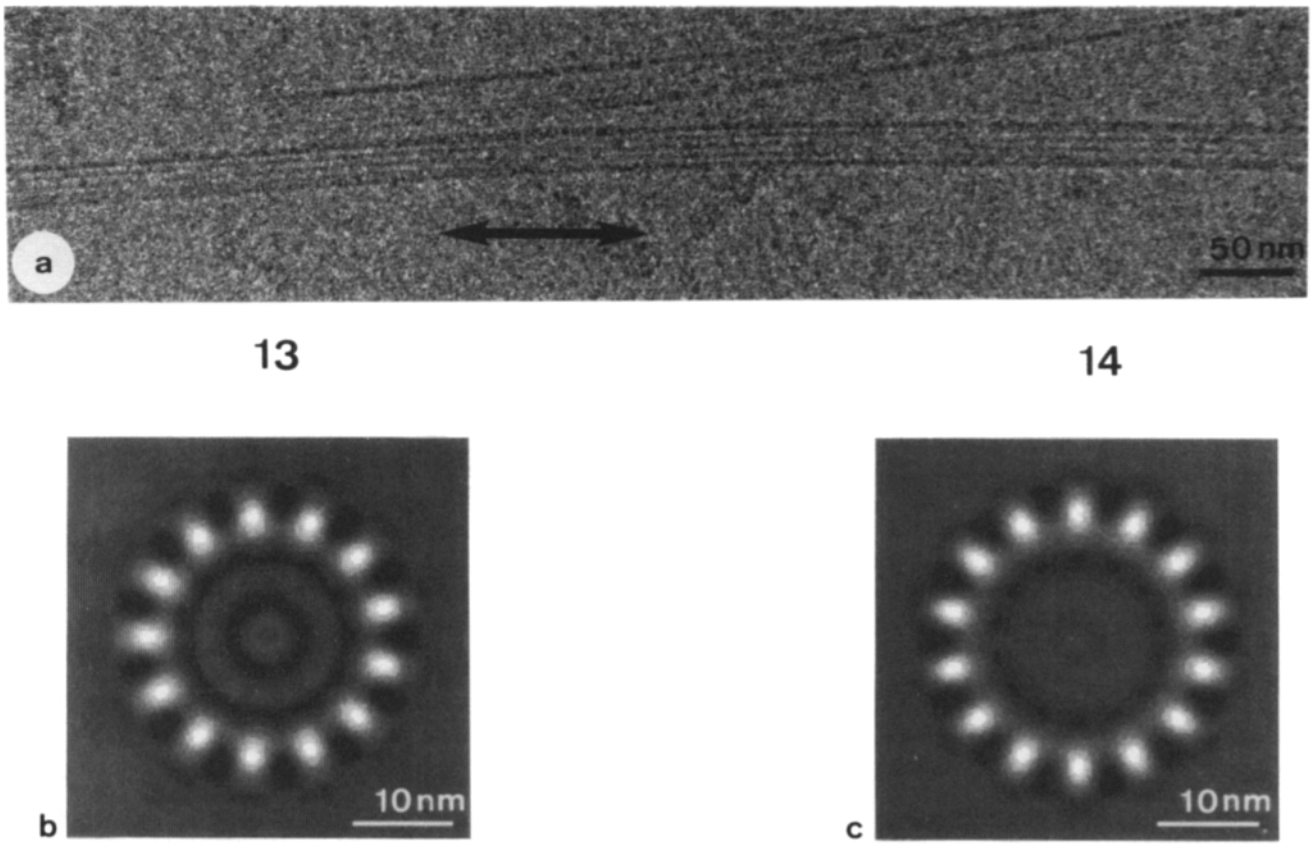

Figure 4. (*a*) Micrograph of a frozen hydrated microtubule with a 13 ⇔ 14 pf transition indicated by the double arrow. Calculated sections corresponding to segments on either side of the transition indicate (*b*) 13 pfs, (*c*) 14 pfs.

finer inner fringes, separated by ~5 nm, whose contrast varies in a characteristic way along the microtubule. The image contrast gives a direct and accurate identification of the number of pfs in each microtubule (11–13, 41). Note that some microtubule images in Fig. 2 show transitions from one of the characteristic contrast patterns to another, (*double arrows*) accompanied by a slight change in image width which can be seen by looking obliquely along these microtubules. These contrast transitions indicate that the pf number varies along the microtubule.

Fig. 3 shows different contrast transitions corresponding to the following changes in pf numbers: 12 ⇔ 13 (Fig. 3 *a*), 13 ⇔ 14 (Fig. 3 *b*), 14 ⇔ 15 (Fig. 3 *e*), and 15 ⇔ 16 (not shown), double increment transitions of the type 11 ⇔ 13 (Fig. 3 *g*), 13 ⇔ 15 (not shown), and 14 ⇔ 16 (Fig. 3 *f*) are also observed. Out of 277 transitions surveyed, 95% involve single pf increments, the remainder correspond to double pf increments. We have also observed several transitions along the same microtubule (Fig. 3 *d*), but the quantification of such events is limited by the available field of view at the working magnification.

A microtubule with a contrast pattern transition is shown at high magnification in Fig. 4 *a*. Cross-sections were calculated from the image segments on either side of the transition, as described in Materials and Methods, using a first estimate of the number of pfs N based on the image contrast. Only one of the calculated cross-sections on each side of the transition turns out to be acceptable. As shown in Fig. 4, *b* and *c*, this transition is of the type 13 ⇔ 14 pfs, substantiating the interpretation based directly on the image contrast. Similar calculations for different types of transition consistently show agreement between pf numbers deduced from the cross-sections and from the image contrast.

To assess whether the presence of transitions depends on either the assembly conditions or assembly time, we followed the evolution of microtubule populations in samples prepared in the presence of 1 and 5 mM magnesium, see Materials and Methods. Transition frequencies and average separations between transitions were estimated as described. The results are presented in Fig. 5. The populations consisted principally of 13, 14, and 15 pf microtubules with small numbers of 11, 12, 16, and 17 pf microtubules and some doublet-like structures. We concentrate here on the major 14 pf component, which for 1 mM magnesium, made up 88% of the population at the early stages of assembly and 83% after one hour. The corresponding average separations between transitions were 23.3 and 20.9 μm, respectively. For 5 mM magnesium there were 75 and 65% of 14 pf microtubules at equivalent early

Figure 3. Micrographs of frozen-hydrated specimens showing images of individual microtubules with contrast transitions (↔) corresponding to changes in the number of pfs. (*a*) Transition 12 ⇔ 13. (*b*) Transition 13 ⇔ 14. (*c*) Transition 13 ⇔ 14 close to microtubule extremity. (*d*) Two closely spaced transitions 12 ⇔ 13 and 13 ⇔ 14. (*e*) Transition 14 ⇔ 15. (*f*) Double increment transition 14 ⇔ 16. (*g*) Double increment transition 11 ⇔ 13 near the microtubule extremity.

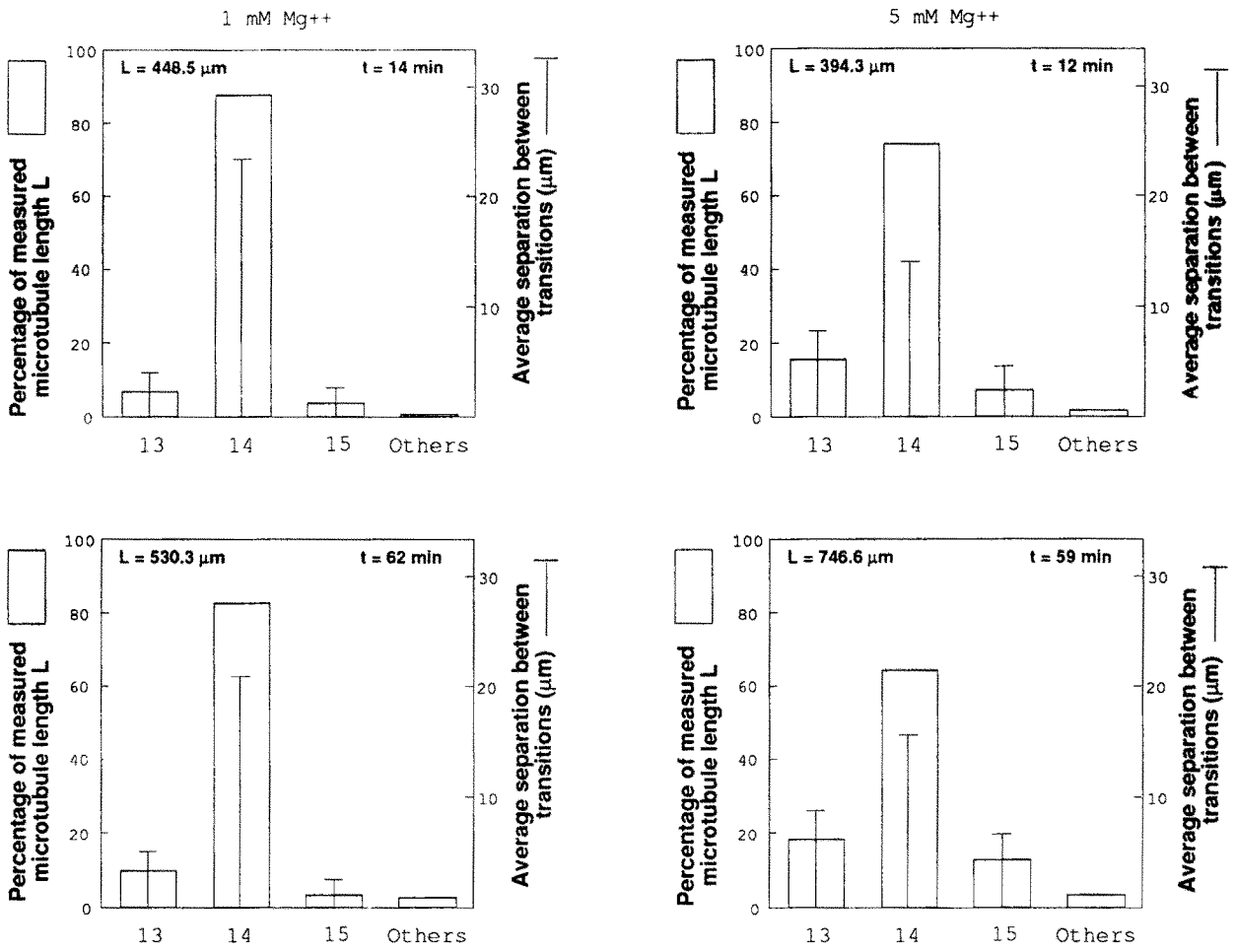

Figure 5. Evolution of pf number distribution with assembly time and with magnesium concentration. (*Left*) Assembly in the presence of 1 mM magnesium. (*Right*) Assembly in the presence of 5 mM magnesium. The time of freezing (t) and the total microtubule length (L) measured from three negatives are indicated in the histograms. Percentages of microtubule length for each pf configuration are indicated by the height of the boxes (left scale). In the assembly conditions used the 13, 14, and 15 pf configurations made up ~90% of the total population. Other minority configurations had 11, 12, 16, and 17 pfs and "doublet-like" structures. The average separations between transitions are indicated by the vertical bars (right scale). The upper-left histogram corresponds to the data summarized in Table II.

and late assembly times, the transition separations were 13 and 16 μm, respectively. The detailed evolution of all components can be followed in Fig. 5.

The most significant difference between the two assembly conditions is the reduction in the average spacing between transitions at 5 mM magnesium, 13 compared to 23 μm. In both cases these spacings were relatively time independent. The two assembly conditions also differ in the time evolution of the microtubule populations. With 1 mM magnesium the population is stable whereas, with 5 mM magnesium, there is a significant reduction in the number of 14 pfs after one hour.

It was not possible to determine the overall length distribution of the microtubules in these samples. Observation at low magnification indicates that on the average the microtubules were longer than 15 μm. Consequently, complete microtubules with uniquely 13 or 15 pfs must be very rare since they have separations between transitions smaller than 15 μm.

Microtubules Assembled in Cell Free Extracts from Xenopus Eggs

To test whether the existence of transitions is limited to microtubules assembled from 3×-tubulin (and phosphocellulose-purified tubulin, data not shown), we analyzed microtubules assembled in concentrated interphasic *Xenopus* egg extracts. The dynamic properties of the microtubules which polymerize in these extracts have been shown to mimic quite well the situation pertaining to interphasic cells (5). Fig. 6 shows microtubules assembled at room temperature in such extracts. Most microtubules show the characteristic 13 pf contrast and other microtubules show the longitudinal contrast repeats typical of 14 and 15 pf microtubules. 12 pf microtubules, not present in this micrograph, are also observed. Table I presents the experimental values of the longitudinal contrast periodicities for these different microtubules. They are found to be close to values obtained previously for microtubules assembled from beef brain tubulin and to the theoretical values deduced from our surface lattice accommodation model (12, 39). This indicates that the structure of the cell extract microtubules is similar to those assembled from purified tubulin.

Protofilament transitions are also observed in the cell extract and are of the type 12 ⇔ 13, 13 ⇔ 14 (*double arrow* in Fig. 6), and 14 ⇔ 15. Table II compares the results obtained from a sample frozen after 5 min assembly at room

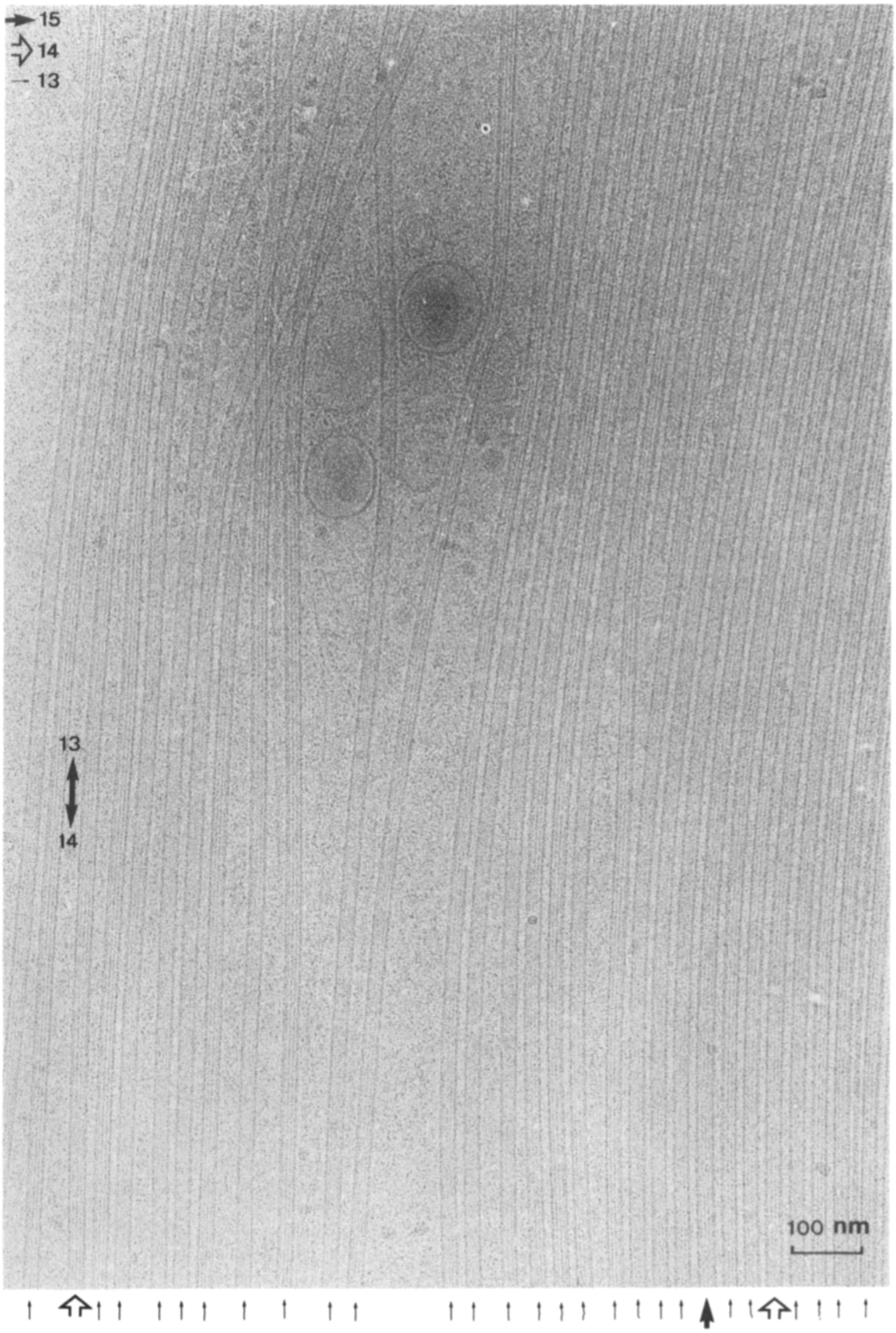

Figure 6. Microtubules in a cell free extract from *Xenopus* eggs. The vast majority of the microtubules are in the 13 pf configuration (→) but 14 (⇨), and 15 (➡) pf microtubules are also observed. A transition of the type 13 ⇔ 14 is indicated by the double arrow. Some vesicles and filamentous structure can be observed.

Table I. Longitudinal Contrast Periodicities of Microtubule Images

Pf number	Experimental values: Cell-free extract	Experimental values: Beef brain tubulin	Theoretical values
	(*nm*)	(*nm*)	(*nm*)
12	381.0	378.0 ± 22.1	344.8
13	several μm	several μm	∞
14	433.7 ± 20.4	415.4 ± 23.3	402.3
15	227.7 ± 6.1	219.3 ± 14.5	215.5

Longitudinal periodicities were measured on enlarged prints. The left and middle column are experimental values obtained from images recorded respectively from cell-free extracts and from purified tubulin assembled in vitro (12). The two data sets are in good agreement and are consistent with the theoretical values deduced from our surface lattice accommodation model (12, 39).

temperature with values for the 3×-tubulin sample after 14 min assembly in the presence of 1 mM magnesium, Fig. 5. In the cell-free extract the microtubule population is essentially 80% 13 pfs, 18% 14 pfs, and 3.5% 15 pfs. The average separation between transitions is 52 μm for 13 pfs, 12 μm for 14 pfs, 4.5 μm for 15 pfs.

Discussion

A range of studies has shown that preservation of macromolecular structures is excellent in vitrified samples (15, 36). Therefore, it is unlikely that the observed dislocations are an artefact of the electron microscope method. Flattening, which occurs when the ice layer is too thin, is observed quite frequently at cross overs between microtubules and is easily recognized (Fig. 2). The use of low dose conditions makes it unlikely that the contrast transitions are produced by radiation damage either. Moreover, in view of the firmly established interpretation of the image contrast (11–13, 41), the observed contrast transitions must be taken to indicate changes in pf number within individual microtubules. These contrast transitions along individual microtubule images are a constant feature of all the in vitro polymerization systems that we have investigated. They are observed in phosphocellulose-purified tubulin and 3×-tubulin microtubules as well as in microtubules assembled in interphasic *Xenopus* egg extracts. Interestingly, the overall image contrasts of microtubules assembled in the egg extracts are similar to those of microtubules assembled from purified microtubule proteins. This is an important observation since it indicates that both types of microtubules have the same basic structure. Changes in pf numbers along a single microtubule have not been directly observed in thin sections, although Böhm et al. (7) suspected that they might occur. It is obviously difficult to detect transitions using thin sectioning since this requires the observation of serial sections of microtubules perfectly aligned in bundles. Our study shows that transitions in pf number occur frequently in microtubules assembled in vitro. The fact that they also occur with a high frequency in microtubules assembled in interphasic egg extracts strongly suggests that they might occur in vivo since the physicochemical conditions found in the cytoplasm of living cells are fairly well reproduced in these extracts.

Table II. Microtubule Population and Transition Frequencies

Pf number	Length (μm)	Percent	Transitions	Frequency (μm^{-1})	Average separation (μm)
3×-tubulin					
13	31.8	7.1	8	0.25	4.0
14	395.6	88.2	17	0.04	23.3
15	18.4	4.1	7	0.38	2.6
Others	2.7	0.6	2	-	-
Cell-free extract					
12	0.4	0.2	1	2.5	0.4
13	207.1	78.7	4	0.02	51.8
14	46.8	17.8	4	0.09	11.7
15	8.9	3.4	2	0.23	4.5

Data on microtubule pf number transitions for a 3×-tubulin sample and a cell-free extract from *Xenopus* eggs. The 3×-tubulin sample was assembled in the presence of 1 mM $MgCl_2$, see Materials and Methods, and prepared for cryo-electron microscopy after 14-min incubation at 37°C. A total microtubule length of 448.5 μm was measured on enlargements of a set of three micrographs. The cell-free extract specimen was prepared after 5-minutes incubation at room temperature. A total microtubule length of 263.2 μm was measured on enlargements of a set of seven micrographs. Transition frequencies and average separation between transitions were calculated as indicated in Materials and Methods.

Are Protofilament Number Transitions Related to the Microtubule Growth Process?

At present, we have no indication of how these defects in the surface lattice organization are generated. We envisage two possibilities: (*a*) they are inherent structural defects generated spontaneously during microtubule growth or; (*b*) they are produced by an end to end annealing process such as that reported to be the major cause of microtubule growth after shearing (32). These possibilities may not be mutually exclusive and it is clear that further work will be necessary to determine the origin of pf number variations. The presence of transitions even when microtubule populations do not evolve in the course of time indicates that they could well be spontaneously produced as errors of microtubule growth. If the number of pfs changes in a single microtubule during its elongation, current concepts concerning microtubule growth will have to be re-examined. Indeed, the usual models involve helical assembly whereas incorporation or substraction of one or two pfs during microtubule growth is more easily understood if tubulin heterodimers first assemble head to tail, forming pfs which then form the microtubule wall by making lateral contacts. Support in favor of this growth mechanism is provided by a recent investigation of frozen hydrated specimens showing that the conformation of microtubule ends differ during the assembly and disassembly phases (23). An intriguing speculation is that the frequency of pf number transitions in microtubules is related in some way to microtubule dynamics. Transitions could be either the cause or the consequence of microtubule dynamics. Such transitions may occur when microtubules alternate between shrinking and growing phases (rescues) in a population undergoing dynamic instability. Along this line, we have observed that for 3×-tubulin, the presence of high magnesium increases the transition frequency in 14 pf microtubules (Fig. 5). This may be compared with the results of O'Brien et al. (28) who used differential interference contrast video light microscopy to study the effects of magnesium on microtubule dynamics. They demonstrated that high magnesium

concentrations increased the dynamic instability of microtubules due to an increase in the transition from the growing to the shrinking phase (catastrophe frequency). However, a clear correlation between microtubule dynamics and the frequency of changes in pf number in microtubules remains to be demonstrated by a quantitative comparison of data obtained by video-microscopy and by cryo-electron microscopy.

What Controls the Structural Fidelity of Microtubules?

Although it is often assumed that in eucaryotic cells, microtubules are composed of 13 pfs (37), this is not always true and cellular microtubules can have a wide range of pf numbers (8, 9), ranging from 11 to 19 (except 18 pfs) in different animal phyla including protozoa (16, 17, 38), nematodes (10, 34), arthropods (14, 25–27, 39), and mammals (33, 42). It has been shown that the pf number may depend on cell type (10), the presence of drugs (26), the cell cycle stage (16, 17), morphogenesis (39), and even on tubulin genes (34). It is entirely unclear why the number of pfs varies like this and how it is regulated in vivo. It is also unclear whether such a variability has a functional meaning. It has been proposed that microtubule pf number is determined by nucleation sites (18, 35). This is certainly true in the case of purified tubulin for which in vitro assembly in the presence of centrosomes gives mostly 13 pf microtubules (18). However, this fidelity may not be absolute since we report here that transitions in pf numbers can occur along the length of a single microtubule. Therefore, it would be interesting to reexamine the frequency of pf number transitions along centrosome-nucleated microtubules. We also report that whereas microtubules assembled from microtubule proteins in the absence of nucleating centers have mostly 14 pfs, those in egg extracts have mostly 13 pfs. A structural polymorphism exists in both cases, with microtubules having different pf numbers, but these are a minority. It is likely that a sizeable fraction of the microtubules with a pf number different from 14 for pure tubulin and from 13 in egg extracts are a result of transitions within single microtubules. In egg extracts, in the absence of added centrosomes, there are no organized nucleation sites since when the extracts are driven into mitosis, there is no spontaneous assembly under conditions where added centrosomes are known to nucleate short microtubule asters (40). Therefore, the 13 pf microtubule configuration observed in egg extracts is probably not imposed by nucleating templates. It would seem that the number of pfs could depend in part on the nucleation event itself and in part on the conditions of the milieu in which the microtubules grow. How this works is still a mystery but it is possible that under specific conditions and in the absence of nucleating templates, the probability of forming a nucleus with N protofilaments is highly favored over other pf numbers. This could then determine the majority pf number in a microtubule population. Numbers other than N may occur because of the low survival frequency of such nuclei or because of the stochastic transitions during elongation mentioned previously.

D. Chrétien thanks the Ministère de la Recherche et de la Technologie and the Région Rhône Alpes for research stipends. We thank C. Closse for expert technical assistance in Grenoble. We are happy to acknowledge help and ready encouragement from Dr. D. Job.

Received for publication 9 October 1991 and in revised form 22 January 1992.

References

1. Aamodt, E. J., and J. G. Culotti. 1986. Microtubules and microtubule-associated proteins from the nematode *Caenorhabditis elegans*: periodic cross-links connect microtubules in vitro. *J. Cell Biol.* 103:23–31.
2. Amos, L. A., and A. Klug. 1974. Arrangement of subunits in flagellar microtubules. *J. Cell Sci.* 14:523–549.
3. Asnes, C. F., and L. Wilson. 1979. Isolation of bovine brain microtubule protein without glycerol: polymerization kinetics change during purification cycles. *Anal. Biochem.* 98:64–73.
4. Beese, L., G. Stubbs, and C. Cohen. 1987. Microtubule structure at 18Å resolution. *J. Mol. Biol.* 194:257–264.
5. Belmont, L. D., A. A. Hyman, K. E. Sawin, and T. J. Mitchison. 1990. Real-time visualization of cell-cycle dependent changes in microtubule dynamics in cytoplasmic extracts. *Cell.* 62:579–589.
6. Binder, L. I., and J. L. Rosenbaum. 1978. The in vitro assembly of flagellar outer doublet tubulin. *J. Cell Biol.* 79:500–515.
7. Böhm, K. J., W. Vater, H. Fenske, and E. Unger. 1984. Effect of microtubule-associated proteins on the protofilament number of microtubules assembled in vitro. *Biochem. Biophys. Acta.* 800:119–126.
8. Burton, P. R., and R. E. Hinkley. 1974. Further electron microscopic characterization of axoplasmic microtubules of the ventral nerve cord of the crayfish. *J. Submicrosc. Cytol.* 6:311–326.
9. Burton, P. R., R. E. Hinkley, and G. B. Pierson. 1975. Tannic acid-stained microtubules with 12, 13 and 15 protofilaments. *J. Cell Biol.* 65:227–233.
10. Chalfie, M., and J. N. Thomson. 1982. Structural and functional diversity in the neuronal microtubules of *Caenorhabditis elegans*. *J. Cell Biol.* 93:15–23.
11. Chrétien, D. 1991. Apports de la cryomicroscopie électronique à l'étude de microtubules assemblés in vitro. Ph.D. Thesis. Université Joseph Fourier, Grenoble, France. 191 pp.
12. Chrétien, D., and R. H. Wade. 1991. New data on the microtubule surface lattice. *Biol. Cell.* 71:161–174.
13. Chrétien, D., D. Job, and R. H. Wade. 1990. Observations of frozen-hydrated microtubules. *In* Proceedings of the XIIth International Congress for electron microscopy. L. D. Peachey, and D. B. Williams, editors. San-Francisco Press, San Francisco, CA. 1:504–505.
14. Dallai, R., and B. A. Afzelius. 1990. Microtubular diversity in insect spermatozoa: results obtained with a new fixative. *J. Struct. Biol.* 103:164–179.
15. Dubochet, J., M. Adrian, J. Lepault, and A. W. McDowall. 1985. Cryo-electron microscopy of vitrified biological specimens. *Trends Biochem. Sci.* 10:143–146.
16. Eichenlaub-Ritter, U. 1985. Spatiotemporal control of functional specification and distribution of spindle microtubules with 13, 14 and 15 protofilaments during mitosis in the ciliate *Nycotherus*. *J. Cell Sci.* 76:337–355.
17. Eichenlaub-Ritter, U., and J. B. Tucker. 1984. Microtubules with more than 13 protofilaments in the dividing nuclei of ciliates. *Nature (Lond.).* 307:60–62.
18. Evans, E., T. Mitchison, and M. Kirschner. 1985. Influence of the centrosome on the structure of nucleated microtubules. *J. Cell Biol.* 100:1185–1191.
19. Deleted in proof.
20. Job, D., M. Pabion, and R. L. Margolis. 1985. Generation of microtubule stability subclasses by microtubule-associated proteins: implications for the microtubule "dynamic instability" model. *J. Cell Biol.* 101:1680–1689.
21. Klug, A., F. H. C. Crick, and H. W. Wyckoff. 1958. Diffraction by helical structures. *Acta Cryst.* 11:199–213.
22. Linck, R. W., and G. L. Langevin. 1981. Reassembly of flagellar B($\alpha\beta$) tubulin into singlet microtubules: consequences for cytoplasmic microtubule structure and assembly. *J. Cell Biol.* 89:323–337.
23. Mandelkow, E.-M., E. Mandelkow, and R. A. Milligan. 1991. Microtubule dynamics and microtubule caps: a time-resolved cryo-electron microscopy study. *J. Cell Biol.* 114:977–991.
24. McEwen, B., and S. J. Edelstein. 1980. Evidence for a mixed lattice in microtubules reassembled in vitro. *J. Mol. Biol.* 139:123–145.
25. Mogensen, M. M., and J. B. Tucker. 1987. Evidence for microtubule nucleation at plasma membrane-associated sites in *Drosophila*. *J. Cell Sci.* 88:95–107.
26. Mogensen, M. M., and J. B. Tucker. 1990. Taxol influences control of protofilament number at microtubule-nucleating sites in *Drosophila*. *J. Cell Sci.* 97:101–107.
27. Nagano, T., and F. Suzuki. 1975. Microtubules with 15 subunits in cockroach epidermal cells. *J. Cell Biol.* 64:242–245.
28. O'Brien, E. T., E. D. Salmon, R. A. Walker, and H. P. Erickson. 1990.

Effects of magnesium on the dynamic instability of individual microtubules. *Biochemistry*. 29:6648–6656.
29. Peterson, G. L. 1979. Review of the Folin phenol quantitation method of Lowry, Rosebrough, Farr and Randall. *Anal. Biochem.* 100:201–220.
30. Deleted in proof.
31. Pierson, G. B., P. R. Burton, and R. H. Himes. 1978. Alterations in number of protofilaments in microtubules assembled in vitro. *J. Cell Biol.* 76:223–228.
32. Rothwell, S. W., W. A. Grasser, and D. B. Murphy. 1986. End-to-end annealing of microtubules in vitro. *J. Cell Biol.* 102:619–627.
33. Saito, K., and K. Hama. 1982. Structural diversity of microtubules in the supporting cells of the sensory epithelium of guinea pig organ of Corti. *J. Electr. Micr.* 31:278–281.
34. Savage, C., M. Hamelin, J. G. Culotti, A. Culson, D. G. Albertson, and M. Chalfie. 1989. *mec-7* is a β-tubulin gene required for the production of 15-protofilament microtubules in *Caenorhabditis elegans*. *Genes and Development*. 3:870–881.
35. Scheele, R. B., L. G. Bergen, and G. G. Borisy. 1982. Control of the structural fidelity of microtubules by initiation sites. *J. Mol. Biol.* 154:485–500.
36. Stewart, M., and G. Vigers. 1986. Electron microscopy of frozen-hydrated biological material. *Nature (Lond.)*. 319:631–636.
37. Tilney, L. G., J. Bryan, D. J. Bush, K. Fujiwara, M. S. Mooseker, D. B. Murphy, and D. H. Snyder. 1973. Microtubules: evidence for 13 protofilaments. *J. Cell Biol.* 59:267–275.
38. Tucker, J. B., S. A. Mathews, K. A. Hendry, J. B. Mackie, and D. L. J. Roche. 1985. Spindle microtubule differentiation and deployment during micronuclear mitosis in *Paramecium*. *J. Cell Biol.* 101:1966–1976.
39. Tucker, J. B., M. J. Milner, D. A. Currie, J. W. Muir, D. A. Forrest, and M.-J. Spencer. 1986. Centrosomal microtubule organizing centres and a switch in the control of protofilament number for cell surface-associated microtubules during *Drosophila* wing morphogenesis. *Eur. J. Cell Biol.* 41:279–289.
40. Verde, F., J.-C. Labbé, M. Dorée, and E. Karsenti. 1990. Regulation of microtubule dynamics by cdc2 protein kinase in cell-free extracts of *Xenopus* eggs. *Nature (Lond.)*. 343:233–238.
41. Wade, R. H., D. Chrétien, and D. Job. 1990. Characterization of microtubule protofilament numbers. How does the surface lattice accommodate? *J. Mol. Biol.* 212:775–786.
42. Xu, Z., and B. A. Afzelius. 1988. Early changes in the substructure of the marginal bundle in human blood platelets responding to adenosine diphosphate. *J. Ultrastruct. Mol. Struct. Res.* 99:254–260.